Supplementary Material: Multiscale carrier-envelope phase characterization of 2-µm pulses delivered by a 200-kHz optical parametric amplifier

Katrin Meier[1], Arvid Klösgen[1], Kerstin Harland[1], Lina Hansen[1], Lars Barnekow[1], Chen Guo[2], Caroline Juliano[2], Jin Niu[2], Cord L. Arnold[2] and Jan Vogelsang[1]

[1]Institute of Physics, Carl von Ossietzky Universität Oldenburg, Germany.
[2]Department of Physics, Lund University, Sweden.

This document provides supplementary information to "Multiscale carrier-envelope phase characterization of 2-µm pulses delivered by a 200-kHz optical parametric amplifier". Additional measurement data are shown to further characterize the signal pulses of the visible non-collinear optical parametic amplifier (NOPA), the idler pulses of the difference-frequency generation (DFG) stage and the amplified pulses when using BiBO as the nonlinear crystal. The temporal structure of the amplified near-infrared (NIR) pulses is further characterized by calculating the Fourier-transformation of the spectrum. Additionally, the procedure for measuring the carrier-envelope phase (CEP) of the output pulses is further explained.

S.1 Temporal characterization of the VIS-NOPA

The signal output pulses of the visible NOPA stage are characterized using an interferometric frequency-resolved autocorrelation (IFRAC) measurement [1]. The NOPA spectrum supports a transform-limited pulse duration of 12.3 fs. The IFRAC trace is shown in Fig. S1(a) together with the retrieved trace (b) with a retrieval trace error of 2.4 %. The retrieved pulse duration is 48.7 fs (d), which corresponds to a pulse duration of 39.0 fs for the pulse itself after subtraction of the phase induced by 1 mm of fused silica at an angle of 45° used as a beamsplitter in the interferometer. The parabolic shape of the phase curve shown in Fig. S1(c) indicates a significant impact of group velocity dispersion GDD. This is further determined by fitting the phase data using a Taylor series around $\lambda_0 = 680$ nm revealing $|GDD| = 560\,\text{fs}^2$.

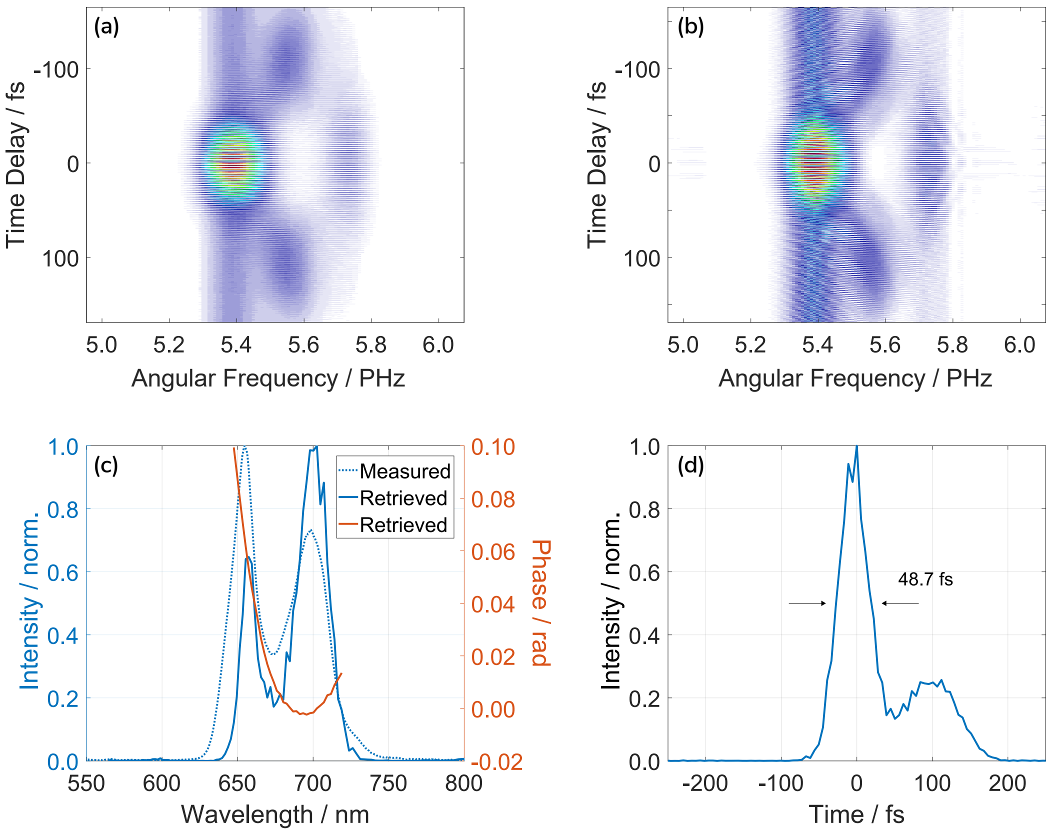

Figure S1: Measured (a) and retrieved (b) IFRAC measurement for the characterization of the NOPA signal (retrieval trace error: 2.4 %) with the additional dispersion of the beamsplitter used in the interferometer (1 mm of fused silica at an angle of 45°) included. The resulting spectral and temporal pulse shape are shown in (c) and (d), respectively.

S.2 Temporal characterization of the DFG idler pulses

The DFG idler pulses before the amplification stage are characterized via third-harmonic generation dispersion-scan (THG d-scan). The result is shown in Fig. S2(a). The main pulse has a FWHM pulse duration of 45 fs, followed by a post-pulse with a relative height of 75 % and a FWHM pulse duration of 55 fs. With the additional material dispersion of the amplifier crystal, the total pulse duration and the duration of each of the two sub-pulses decrease. This is also illustrated in Fig. S2(b). When propagating through the BBO crystal, the relative height of the post-pulse decreases to 70 % and the temporal FWHM of the main pulse decreases to 25 fs. In the BiBO crystal, the relative height of the post-pulse decreases to 60 % and the temporal FWHM of the main pulse decreases to 25 fs.

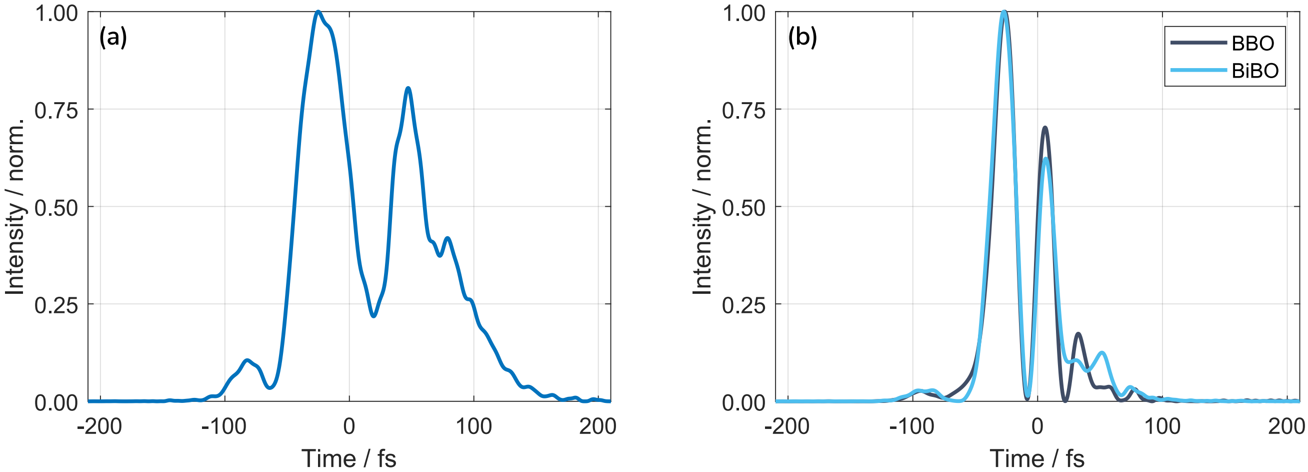

Figure S2: Pulse duration of the DFG pulses (a) before the amplification stage, measured via THG d-scan, and (b) after calculated propagation through 4 mm of BBO/BiBO.

S.3 Temporal characterization of the NIR pulses amplified in BiBO

The NIR pulses after amplification in BiBO are also characterized via THG d-scan. The result is shown in Fig. S3(a). The normalized RMS trace error for the retrieval is 1.5 %. As in the case of BBO, the dip in the middle of the spectrum is visible, as well as the correlated lower-intensity side pulses in the time domain, each with a peak intensity of about 25 % of the pulse peak intensity. The main pulse has a FWHM duration of 18.1 fs, which is close to the transform-limited pulse duration of 16.7 fs.

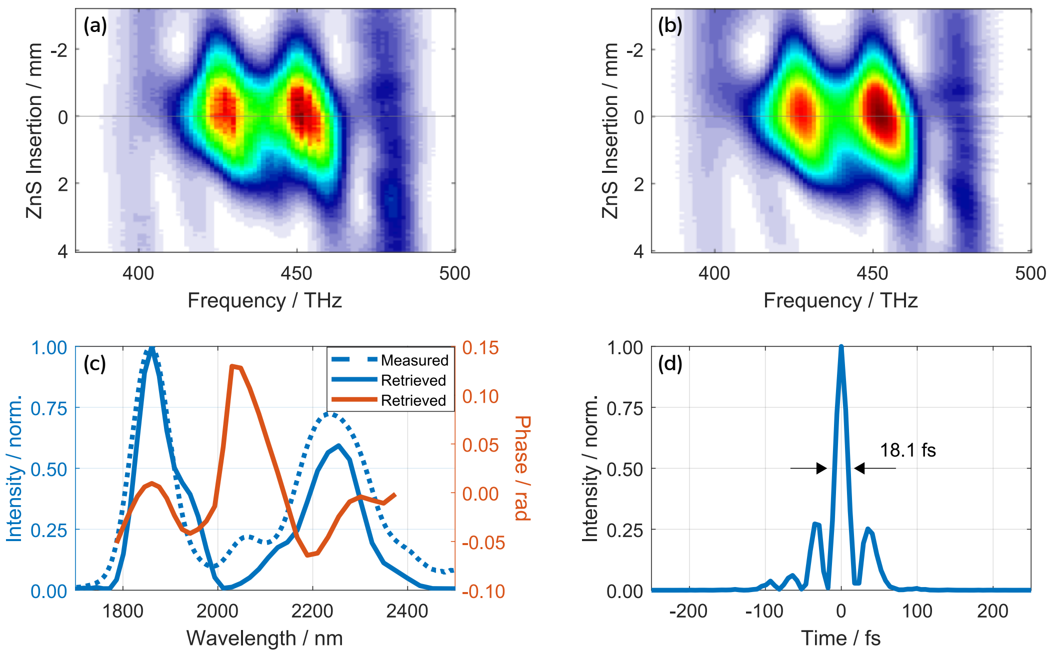

Figure S3: (a) Measured and (b) retrieved d-scan trace of the NIR pulses amplified in BiBO (retrieval trace error: 1.5 %). (c) Measured fundamental spectrum and reconstructed spectral intensity and phase. (d) Resulting temporal structure, revealing a short main pulse with a temporal FWHM duration of 18.1 fs, surrounded by lower-intensity side pulses.

S.4 Transform-limited pulse duration of the amplified pulses

The temporal shape of the amplified pulses exhibits symmetric, lower-intensity pre- and post-pulses. This relates to the shape of the fundamental spectrum, specifically the dip in the middle at around 2 µm. This is illustrated by computing the temporal structure of a pulse with the measured spectral intensity and a flat spectral phase:

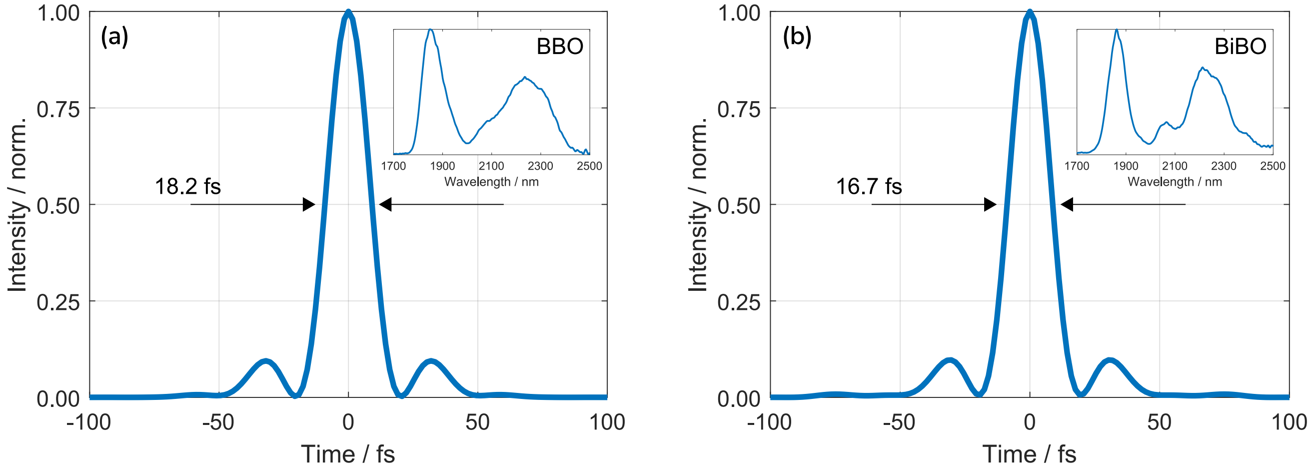

Figure S4: Calculated temporal pulse structure for a laser pulse with the measured spectrum (inset) and a flat phase for (a) amplification in BBO and (b) in BiBO.

S.5 Simulation of the amplification in BBO

The parametric amplification process is simulated using the SISYFOS code package [2]. A complete experimental dataset including input and output pulse energies, spot sizes, spectra and temporal pulse structures is collected prior to running the simulation. The simulated output spectrum compared to the measured one is shown in Fig. S5.

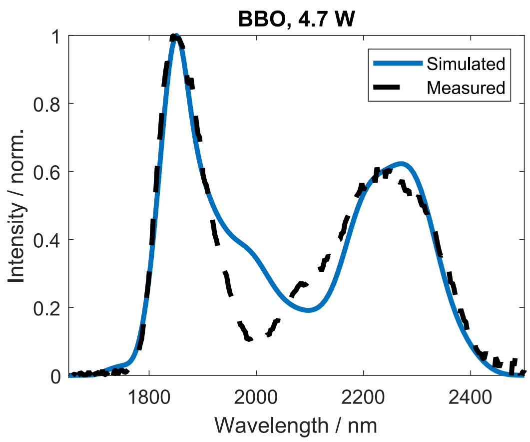

Figure S5: Simulated output spectrum with a simulated output power of 4.7 W in comparison to the measured output spectrum with a power of 4.4 W after amplification in BBO.

S.6 Investigation of the CEP stability of the laser system

The CEP of the output pulses is measured using a home-built f-$2f$-interferometer. It consists of a white light generation part and subsequent frequency doubling of the broadened spectrum, both producing spectral components in the region around 700-800 nm. The relative intensity of these components is adjusted using a polarizer. The resulting spectral interference pattern averaged over 200 pulses and recorded for seven minutes is shown in Fig. S6(a). An exemplary spectrum from the beginning of the measurement is shown in Fig. S6(b).

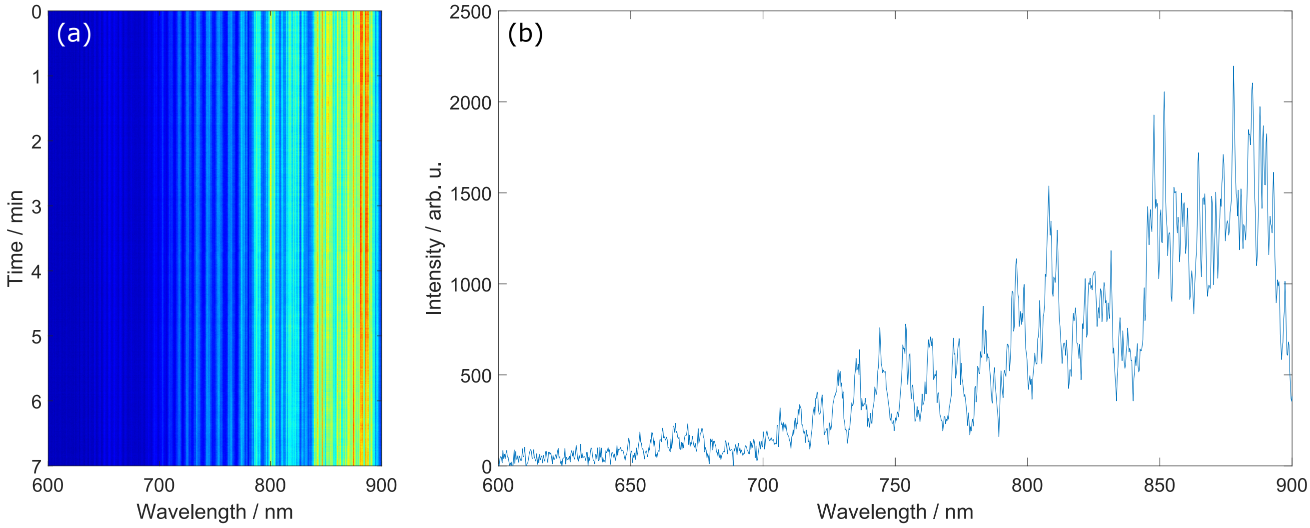

Figure S6: Investigation of the CEP stability of the laser system. (a) Interference pattern recorded with an f-$2f$-interferometer averaged over 200 pulses and measured over seven minutes. (b) Exemplary spectrum from the dataset shown in (a). The phase of the fringe oscillation is extracted at the peak of the Fourier-transform of the signal in the spectral region of 700-800 nm.

A possible correlation between the measured CEP oscillations and the pulse energy stability is investigated by measuring both simultaneously on a shot-to-shot basis. The result is shown in Fig. S7, which reveals no direct correlation between the two quantities. Additionally, a calculated cross-correlation revealed no evident connection. The recorded pulse energy stability over the measurement time frame is 1.6 %, which is higher than the value reported in the main manuscript. This discrepancy is due to suboptimal measurement conditions in a preliminary setup used here. Small beam pointing instabilities will most likely have influenced the pulse energy determination, which is why the dataset actually includes both pulse energy and beam pointing variations. No correlation is found, but a more detailed investigation with a separate measurement of all relevant parameters might be interesting to look at in the future. The impact of a shutter used to synchronize the measurements can be seen in the values for the final pulses.

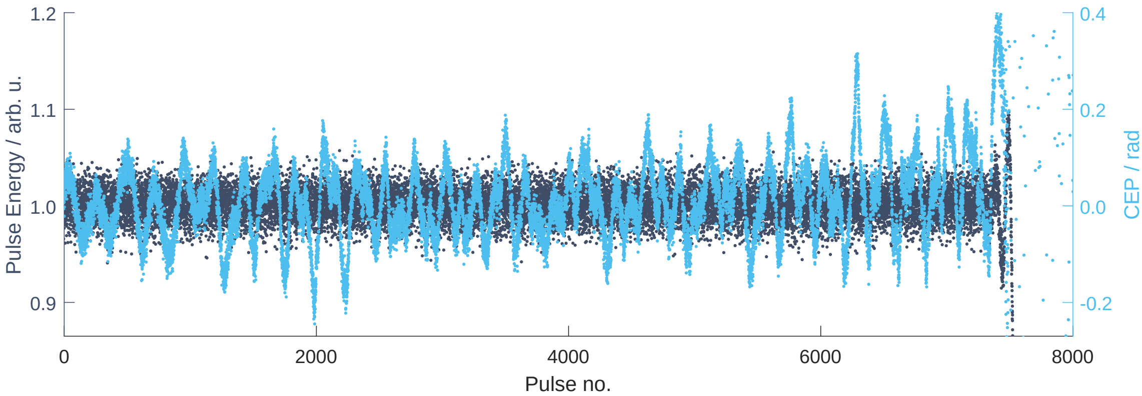

Figure S7: Comparison of the CEP stability and the pulse energy stability.

References

[1] G. Stiben and G. Steinmeyer. Interferometric frequency-resolved optical gating. *Optics Express*, 13:2617, 2005. doi: 10.1364/OPEX.13.002617.

[2] G. Arisholm and H. Fonnum. Simulation System For Optical Science (SISYFOS) – tutorial, version 2. https://www.ffi.no/en/publications-archive/simulation-system-for-optical-science-sisyfos-tutorial-version-2, 2021.